

# Resistance to sulfur poisoning of Ni-based alloy with coinage (IB) metals



Xiaopei Xu<sup>a</sup>, Yanxing Zhang<sup>a</sup>, Zongxian Yang<sup>a,b,\*</sup>

<sup>a</sup> College of Physics and Electronic Engineering, Henan Normal University, Xinxiang, Henan 453007, China

<sup>b</sup> Collaborative Innovation Center of Nano Functional Materials and Applications, Kaifeng, Henan, China

## ARTICLE INFO

### Article history:

Received 8 August 2015

Received in revised form 9 October 2015

Accepted 10 October 2015

Available online 22 October 2015

### Keywords:

Solid oxide fuel cell

Sulfur poisoning

Ni Anode

IB metal

## ABSTRACT

The poisoning effects of S atom on the (1 0 0), (1 1 0) and (1 1 1) metal surfaces of pure Ni and Ni-based alloy with IB (coinage) metals (Cu, Ag, Au) are systematically studied. The effects of IB metal dopants on the S poisoning features are analyzed combining the density functional theory (DFT) results with thermodynamics data using the ab initio atomistic thermodynamic method. It is found that introducing IB doping metals into Ni surface can shift the d-band center downward from the Fermi level and weaken the adsorption of S on the (1 0 0) and (1 1 0) surfaces, and the S tolerance ability increases in the order of Ni, Cu/Ni, Ag/Ni and Au/Ni. Nevertheless, on the (1 1 1) surface, the S tolerance ability increases in the order of Ag/Ni (or Cu/Ni), Ni, and Au/Ni. When we increase the coverage of the IB metal dopants, we found that not only Au, but Cu and Ag can increase its S tolerance. We therefore propose that alloying can increase its S tolerance and alloying with Au would be a better way to increase the resistance to sulfur poisoning of the Ni anode as compared with the pure Ni and the Ag- or, Cu-doped Ni materials.

© 2015 Elsevier B.V. All rights reserved.

## 1. Introduction

Solid oxide fuel cells (SOFCs) are expected to be a crucial technology in future power generation [1,2]. SOFCs offer many desirable advantages compared to other types of fuel cells and conversion devices, due to their use of solid electrolytes, lack of moving parts, ability to circumvent precious metal use, high efficiency, low pollution, and fuel flexibility.

However, a major issue in the long-term stability and activity of the anode catalyst is its poor resistance toward poisonous compounds presenting in the feed stream. Trace amounts of H<sub>2</sub>S presenting in biomass generated syngas streams are enough to deactivate the catalyst [3,4]. Liu et al. [5,6] showed that sulfur poisoning observed in the low concentration of H<sub>2</sub>S at elevated temperatures originates from the dissociation of sulfur-containing species and the adsorption of atomic sulfur on the anode surface. The adsorbed H<sub>2</sub>S on Ni surfaces has been shown to be dissociated above 300 K [7], with only S remaining on the surface. The strongly adsorbed S species block the active sites on the anode surface and thus increase the resistance to electrochemical oxidation of the fuel.

To improve the sulfur tolerance of SOFCs, the de-sulfurization of various materials has been extensively studied via experimental and computational approaches, including pure metals (Ni [8–10]) and metal alloys [11–14]. It was found that Au, Ag, Cu, Al, Bi, Cd, Sb, Sn, Zn additions can increase sulfur tolerance of Ni. Copper/ceria/zirconia [15] anodes were reported to be stable in fuel gases containing up to 450 ppm H<sub>2</sub>S. Other anode compositions include a lanthanum doped strontium titanate [16], lanthanum molybdate [17], Pd impregnated titanate/cerate composition [18], gold/molybdenum disulfide [19], and Ni/YSZ modified with niobia [20] showed good sulfur tolerance.

Several research groups have modeled M/Ni (M is one of typical transition metals of Cu, Fe, Co, etc.) surfaces as Ni supercell slabs with the alloying atoms in each slab layer [3,6,21]. It was reported by Christensen et al. [22] that metals such as Ag and Au on Ni substrate have shown negative values of parameters segregation energy and positive values of surface mixing energy, indicating that the deposited metal prefers to stay on the Ni surface without the formation of subsurface alloy or separate islands. These theoretical predictions agree well with experimental observations. It has been found in STM studies by Nielsen et al. [23] that when Au is added to any of the low index Ni surfaces, an alloy is formed in the first atomic layer. Vahalia [24] investigated Ni<sub>83</sub>Cu<sub>17</sub> alloy by using X-ray photoelectron spectroscopy technique, and reported that Cu was strongly segregated on the top (1 0 0) and (1 1 1) surfaces at 800 K. Sakurai et al. [25] investigated the surface segregation of Cu

\* Corresponding author at: College of Physics and Electronic Engineering, Henan Normal University, Xinxiang, Henan 453007, China.

E-mail address: [yzx@henannu.edu.cn](mailto:yzx@henannu.edu.cn) (Z. Yang).

for Ni<sub>44</sub>Cu<sub>56</sub> alloy by using atom probe technique, and reported that the top five surface layers were pure Cu due to its strong surface segregation at 920 K.

It should be noted that similar model was used for designing surface alloys for steam reforming [26,27]. Experimentally, it has been found that alloying the nickel catalyst with IB-group metals can largely eliminate the carbon deposition [28–30]. Despite these studies, the mechanism of the above experimental observations still needs to be clarified and theoretical analysis can help in this respect.

Herein, we comprehensively simulate the adsorption of S atom on the pure Ni (1 0 0), (1 1 0) and (1 1 1) metal surfaces. The effects of IB metal dopants (Cu, Ag, Au) in the Ni surfaces on the S poisoning features are studied combining the DFT results with thermodynamics data using the ab initio atomistic thermodynamic method.

## 2. Model and computation method

The calculations are performed using spin-polarized periodic DFT as implemented in the Vienna ab initio simulation package (VASP) [31]. Specifically, the exchange correlation functional with generalized gradient approximation (GGA) of Perdew, Burke, and Ernzerhof (PBE) [32] combined with the projector-augmented wave (PAW) [33] method is used to solve the Kohn–Sham equations. The Kohn–Sham orbitals are expanded in plane-wave basis sets with a well-converged cut-off energy 400 eV. The surfaces are modeled by supercells comprising of a four-layer slab with a (2 × 2) lateral replication in the *x*–*y* plane.

A vacuum layer of 10 Å along the *z* direction placed between the slabs to wipe out any spurious interactions between two periodic images. We had checked the vacuum layer before our systematic calculations. For example, we have checked the adsorption energy of S adsorption on the (1 0 0), (1 1 0) and (1 1 1) surfaces of pure Ni and Ni-based alloy with IB metals (Cu, Ag, Au) dopants with 15 Å vacuum layer. The results are shown in Table S1 of the supporting information. Obviously, the larger vacuum layer has scarcely any influence on the calculated results as compared with those for the vacuum layer of 10 Å. For the most stable chemisorption configurations on the surface, the differences in  $E_{ads}$  are less than 0.01 eV. Therefore, the vacuum layer of 10 Å should be enough.

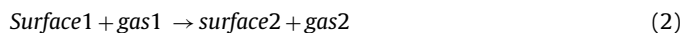
The atoms in the lower two layers are fixed at their equilibrium bulk phase positions, with a lattice constant of 3.52 Å, while those in the upper two layers are allowed to relax. The M/Ni (M = Cu, Ag, Au) surface alloy model is constructed by replacing one of the Ni atoms in the topmost layer with an M atom (i.e., at the M coverage of 0.25 ML). To clarify the stability of surface doping, we studied segregation of the alloying additions at Ni(1 0 0), Ni(1 1 0) and Ni(1 1 1) surfaces. For this purpose, we calculated the segregation energy as a difference of energies for two systems with the doping atom placed at the surface layer and at the central layer (2nd layer in this study), respectively. The results are listed in Table S2 of the supporting information. The negative segregation energy indicates that the doping atoms tend to segregate to the Ni surface. The Brillouin-zone (BZ) integration is performed using the Gaussian smearing method [34] with a finite temperature width of 0.2 eV in order to improve convergence of states near the Fermi level. The *k*-points are sampled in the BZ with a 4 × 4 × 1 *k*-point mesh generated via the Monkhorst–Pack scheme [35]. The conjugate gradient algorithm is used in the optimization, providing a convergence of 1.0 × 10<sup>−5</sup> eV atom<sup>−1</sup> in energies and 0.01 eV Å<sup>−1</sup> in Hellmann–Feynman force on each atom. The energy of an isolated molecule is simulated using a cubic cell of 10 × 10 × 10 Å<sup>3</sup>.

The adsorption energy ( $E_{ads}$ ) is calculated using a formula of

$$E_{ads} = E_{ad/sub} - E_{ad} - E_{sub}, \quad (1)$$

where  $E_{ad}$ ,  $E_{sub}$ , and  $E_{ad/sub}$  are the total energies of the optimized adsorbate in the gas phase, the clean substrate, and the adsorbate/substrate system, respectively. A negative  $E_{ads}$  represents an exothermic adsorption, and the smaller  $E_{ads}$  means the stronger binding of the adsorbate to the surface.

Considering the effect of temperature and partial pressure of various gases, we calculated the Gibbs free energy  $G(T, p)$  of the whole system. According to previously reported works [6,36,37], for a gas-surface interfacial reaction:



where *surface1* and *surface2* represent the reactant and product, respectively, in the condense phase, whereas *gas1* and *gas2* correspond to the reactant and product, respectively, in the gas phase.

The change of Gibbs free energy ( $\Delta G(T, P)$ ), as functions of temperature (*T*) and total pressure (*P*), for reaction (2) can be expressed as:

$$\Delta G(T, P) = (G_{\text{surface2}}(T, P) - G_{\text{surface1}}(T, P)) + (G_{\text{gas2}}(T, P) - G_{\text{gas1}}(T, P)) \quad (3)$$

For the Gibbs free energy of the solid phase:

$$G_{\text{surface2}} - G_{\text{surface1}} = (E_{\text{surface2}}^{\text{DFT}} - E_{\text{surface1}}^{\text{DFT}}) + (F_{\text{surface2}}^{\text{vib}} - F_{\text{surface1}}^{\text{vib}}) \quad (4)$$

It has been proven [38] that the Gibbs free energies of surfaces have relatively small variation, <10 meV, in a wide range of temperature (<1500 K) and pressure (<100 atm) and the vibrational and entropic contributions to Gibbs free energies of atomic adsorbates are negligible. Therefore, the Gibbs free energies of solid phases can be approximated by the internal energy computed from DFT calculations.

$$G_{\text{surface}}(T, P) \approx G_{\text{surface}}(0, 0) = E_{\text{surface}}^{\text{DFT}} \quad (5)$$

The Gibbs free energy of a gas phase molecule is strongly affected by both temperature and pressure and can be expressed as:

$$G_{\text{gas}}(T, P) = G_{\text{gas}}(0, 0) + \Delta G_{\text{gas}}(0 \rightarrow T, P^0) + \Delta G_{\text{gas}}(T, P^0 \rightarrow P) \\ = E_{\text{gas}}^{\text{DFT}} + u_{\text{gas}}(T, P^0) + K_B T \ln(P_{\text{gas}}/P^0) \quad (6)$$

Here, the first term is directly from DFT calculations. The second term, chemical potential, which can be found in the empirical thermodynamic database [39], is the standard enthalpies of the gas phase molecules contributing from rotations, vibrations, and ideal-gas entropy at standard pressure ( $P^0$ ) and is temperature-dependent. The third term is a partial pressure-dependent function from Maxwell relation (where  $K_B$  is Boltzmann constant).

So, Eq. (3) can be expressed as:

$$\Delta G(T, P) = (E_{\text{surface2}}^{\text{DFT}} - E_{\text{surface1}}^{\text{DFT}}) + (E_{\text{gas2}}^{\text{DFT}} - E_{\text{gas1}}^{\text{DFT}}) + (u_{\text{gas2}} - u_{\text{gas1}}) \\ + K_B T \ln(P_{\text{gas2}}/P_{\text{gas1}}) \quad (7)$$

The phase boundary can be determined by the equilibrium condition of  $\Delta G(T, P) = 0$ .

## 3. Results and discussion

### 3.1. The adsorption of sulfur on the Ni(1 0 0), Ni(1 1 0) and Ni(1 1 1) surfaces

The most favorable adsorption sites of S on various Ni surfaces are revealed by considering all possible adsorption sites of corresponding surface and are characterized with the smallest

Download English Version:

<https://daneshyari.com/en/article/5356266>

Download Persian Version:

<https://daneshyari.com/article/5356266>

[Daneshyari.com](https://daneshyari.com)